# Supplementary Tables

**Supplementary Table 1.** Face-sensitive ROIs. Mean and range of the cluster peaks for each face ROI identified in the HCP working memory tfMRI task (with the contrast of 'face > other categories')

| Face ROIs | MNI coordinates | | | | | | | | |
|---|---|---|---|---|---|---|---|---|---|
| | Hemisphere | N | x | y | z | x-range | y-range | z-range | ES* |
| **EVC** | R | 677 | 13 | -92 | -3 | 1-28 | -104 to -79 | -16 to 14 | 5.85 |
| | L | 676 | -10 | -93 | -5 | -26 to 0 | -105 to -75 | -16 to 20 | 5.89 |
| **OFA** | R | 680 | 40 | -77 | -11 | 30-54 | -93 to -63 | -20 to -1 | 11.65 |
| | L | 680 | -39 | -78 | -12 | -53 to -26 | -93 to -63 | -20 to 1 | 10.82 |
| **FFA** | R | 680 | 42 | -53 | -18 | 32-52 | -70 to -34 | -28 to -4 | 13.22 |
| | L | 680 | -40 | -53 | -18 | -52 to -30 | -72 to -35 | -29 to -5 | 11.82 |
| **ATL** | R | 678 | 36 | -6 | -37 | 26-49 | -20 to 11 | -49 to -22 | 6.63 |
| | L | 678 | -36 | -6 | -36 | -49 to -24 | -23 to 12 | -50 to -22 | 6.12 |
| **STS** | R | 680 | 53 | -50 | 12 | 39-69 | -68 to -30 | -1 to 26 | 8.68 |
| | L | 680 | -54 | -51 | 12 | -68 to -39 | -69 to -29 | -1 to 28 | 6.86 |
| **IFG** | R | 677 | 48 | 23 | 19 | 32-62 | 5-40 | 5-35 | 5.21 |
| | L | 672 | -46 | 21 | 18 | -57 to -32 | 4-46 | 3-28 | 4.75 |
| **AMG** | R | 678 | 21 | -4 | -19 | 14-32 | -8 to 2 | -32 to -12 | 5.58 |
| | L | 678 | -20 | -4 | -20 | -32 to -14 | -8 to 2 | -30 to -14 | 5.19 |
| **OFC** | R | 678 | 6 | 47 | -15 | 1-14 | 29-60 | -26 to -5 | 6.12 |
| | L | 678 | -6 | 46 | -17 | -16 to -1 | 26-60 | -27 to -5 | 6.16 |
| **PCC** | R | 678 | 6 | -58 | 31 | 2-13 | -72 to -44 | 19-49 | 5.96 |
| | L | 678 | -5 | -58 | 33 | -13 to 0 | -72 to -36 | 19-50 | 5.61 |

*Effect size (ES) represents the mean signal change in the ROI (z-score from the peak voxel) across all subjects. At each individual level, any ROIs with weak responses to face stimuli (i.e. EC<2) would be excluded for subsequent analyses. That's why some ROIs' N was smaller than 680. In sum, only 667 out of 680 subjects had all 18 face ROIs.

EVC: early visual cortex; OFA: occipital face area; FFA: fusiform face area; ATL: anterior temporal lobe; STS: superior temporal sulcus; IFG: inferior frontal gyrus; AMG: amygdala; OFC: orbitofrontal cortex; PCC: posterior cingulate cortex

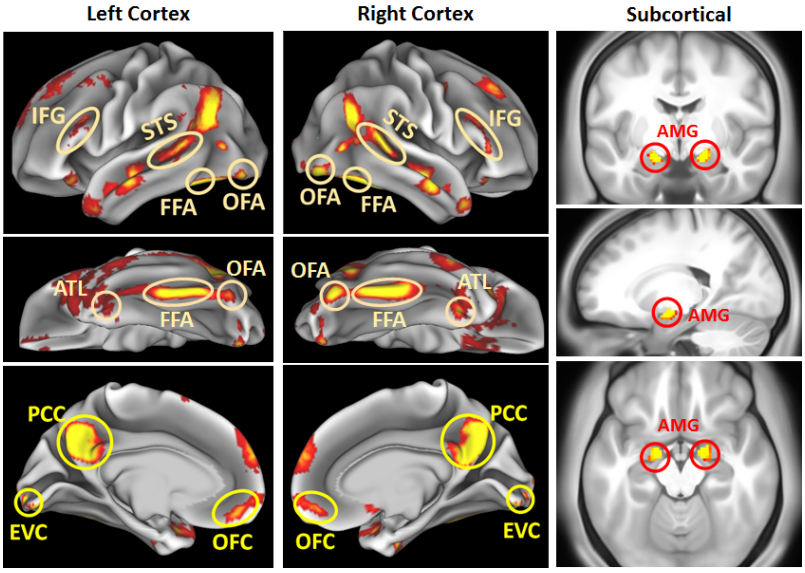


The spatial locations of each face ROI at the group-level. This group-level activation is only for illustration purpose. In fact, we independently defined each face ROI for each subject.

**Supplementary Table 2.** Hemispheric asymmetry of the face connectome at each level of measurements.

| | Right hemisphere predominance | Left hemisphere predominance |
|---|---|---|
| **Neural activation** | **STS** (t=16.31, p<0.001, d=0.63, 95% CI: 1.573, 2.003)<br>**FFA** (t=8.45, p<0.001, d=0.33, 95% CI: 1.069, 1.717)<br>**IFG** (t=6.89, p<0.001, d=0.27, 95% CI: 0.328, 0.590)<br>**ATL** (t=5.68, p<0.001, d=0.22, 95% CI: 0.335, 0.689)<br>**PCC** (t=5.79, p<0.001, d=0.22, 95% CI: 0.228, 0.462)<br>**OFA** (t=5.43, p<0.001, d=0.21, 95% CI: 0.542, 1.156)<br>**AMG** (t=4.61, p<0.001, d=0.18, 95% CI: 0.162, 0.402) | |
| **Structural connectivity** | **AMG connections**<br>**STS-AMG** (t=7.62, p<0.001, d=0.29, 95% CI: 0.011, 0.019)<br>**AMG-OFC** (t=4.39, p<0.001, d=0.17, 95% CI: 0.012, 0.031)<br>**AMG-IFG** (t=2.94, p=0.003, d=0.11, 95% CI: 0.002, 0.011)<br>**OFC connections**<br>**STS-OFC** (t=5.41, p<0.001, d=0.21, 95% CI: 0.004, 0.008)<br>**ATL-OFC** (t=4.87, p<0.001, d=0.19, 95% CI: 0.005, 0.013)<br>**IFG-OFC** (t=4.15, p<0.001, d=0.16, 95% CI: 0.002, 0.005)<br>**STS connections**<br>**STS-ATL** (t=3.06, p=0.002, d=0.12, 95% CI: 0.004, 0.016)<br>**OFA-STS** (t=2.86, p=0.004, d=0.11, 95% CI: 0.002, 0.010)<br>**EVC-STS** (t=2.45, p=0.015, d=0.09, 95% CI: 0.001, 0.006) | **IFG connections**<br>**ATL-IFG** (t=11.65, p<0.001, d=0.45, 95% CI: 0.011, 0.015)<br>**OFA-IFG** (t=8.95, p<0.001, d=0.35, 95% CI: 0.002, 0.003)<br>**FFA-IFG** (t=8.86, p<0.001, d=0.34, 95% CI: 0.005, 0.008)<br>**STS-IFG** (t=5.41, p<0.001, d=0.21, 95% CI: 0.039, 0.083)<br>**PCC connections**<br>**FFA-PCC** (t=7.14, p<0.001, d=0.28, 95% CI: 0.004, 0.008)<br>**OFA-PCC** (t=5.20, p<0.001, d=0.20, 95% CI: 0.003, 0.007)<br>**STS-PCC** (t=3.18, p=0.002, d=0.12, 95% CI: 0.004, 0.016) |
| **Resting-state functional connectivity** | **FFA connections**<br>**FFA-STS** (t=9.52, p<0.001, d=0.37, 95% CI: 0.094, 0.142)<br>**FFA-ATL** (t=4.66, p<0.001, d=0.18, 95% CI: 0.016, 0.038)<br>**FFA-PCC** (t=3.36, p=0.001, d=0.13, 95% CI: 0.011, 0.043)<br>**OFA connections**<br>**OFA-STS** (t=6.50, p<0.001, d=0.25, 95% CI: 0.064, 0.119)<br>**OFA-FFA** (t=6.31, p<0.001, d=0.24, 95% CI: 0.075, 0.143)<br>**OFA-IFG** (t=3.53, p<0.001, d=0.14, 95% CI: 0.016, 0.054)<br>**OFC connections**<br>**AMG-OFC** (t=3.21, p=0.001, d=0.12, 95% CI: 0.008, 0.033)<br>**PCC-OFC** (t=3.03, p=0.003, d=0.12, 95% CI: 0.018, 0.085)<br>**OFA-OFC** (t=2.88, p=0.004, d=0.11, 95% CI: 0.006, 0.031) | **IFG-OFC** (t=3.95, p<0.001, d=0.15, 95% CI: 0.019, 0.055)<br>**EVC-AMG** (t=2.46, p=0.014, d=0.10, 95% CI: 0.003, 0.029) |
| **Effective connectivity** | **Feed-forward connections**<br>**IFG→OFC** (t=2.85, p=0.005, d=0.11, 95% CI: 0.028, 0.152)<br>**STS→AMG** (t=2.71, p=0.007, d=0.10, 95% CI: 0.023, 0.143)<br>**EVC→OFA** (t=2.02, p=0.044, d=0.08, 95% CI: 0.002, 0.144)<br>**FFA→AMG** (t=2.06, p=0.040, d=0.08, 95% CI: 0.003, 0.120)<br>**Feed-back connections**<br>**OFA→EVC** (t=3.14, p=0.002, d=0.12, 95% CI: 0.042, 0.180)<br>**FFA→EVC** (t=3.04, p=0.002, d=0.12, 95% CI: 0.036, 0.168)<br>**STS→OFA** (t=2.96, p=0.003, d=0.11, 95% CI: 0.034, 0.172)<br>**IFG→FFA** (t=2.86, p=0.004, d=0.11, 95% CI: 0.030, 0.161)<br>**OFC→IFG** (t=2.49, p=0.013, d=0.10, 95% CI: 0.017, 0.145)<br>**FFA→OFA** (t=2.38, p=0.018, d=0.09, 95% CI: 0.014, 0.145)<br>**PCC→EVC** (t=2.02, p=0.044, d=0.08, 95% CI: 0.002, 0.134) | |

# Supplementary Figures

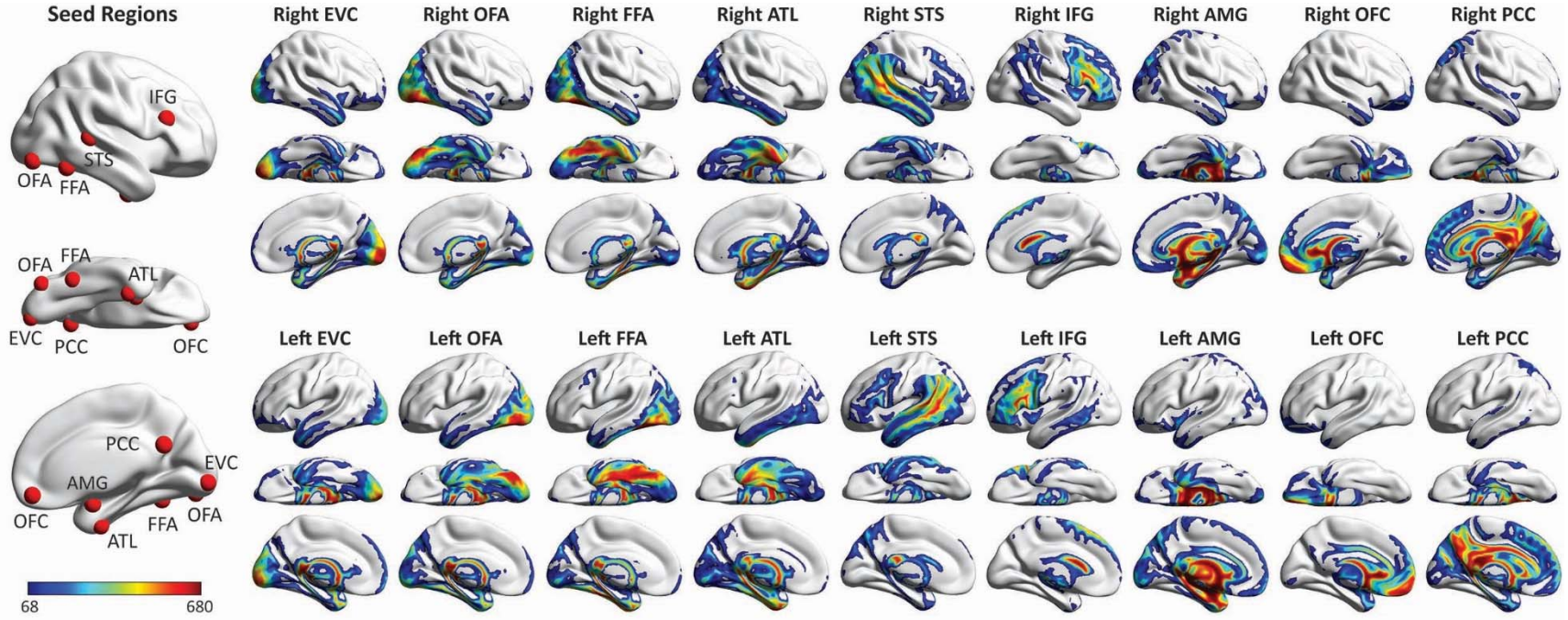


**Supplementary Figure 1. Cortical Projection Zones from Each Face ROI**. For illustrative purpose, the endpoints of streamlines sent from each face ROI were rendered on the ipsilateral cortical surface abutting the white matter. Each subject's cortical projection probabilistic map was firstly thresholded to reduce false-positive fiber tracks (see methods section) and the subject-level binary maps were subsequently aggregated at the group level across all 680 subjects. Color range indicates the degree of between-subject overlap and only voxels with >10% between-subject convergence (i.e. 68 subjects) are showed here. Therefore, the color of each voxel descriptively indicates how many subjects had cortical projection to that voxel in common. Upper row: lateral views. Middle row: ventral views. Lower row: medial views. Besides predominant connections with neighboring areas (proximity bias), each ROI displayed additional projections to a few distant areas. For example, posterior face ROIs (EVC, OFA and FFA) showed consistent projections to ventral temporal areas as well as more anterior regions in temporal pole (ATL). STS showed minimal projections to occipital cortex (OFA) or fusiform gyrus (FFA) but large connections with more distant areas in temporal pole (ATL) and lateral frontal cortex (IFG). Medial ROIs (AMG, OFC and PCC) only showed projections to midline structures. In addition, most face ROIs (except IFG) seemed to have direct fiber projections from early visual cortex.

Abbreviations: EVC: early visual cortex; OFA: occipital face area; FFA: fusiform face area; ATL: anterior temporal lobe; STS: superior temporal sulcus; IFG: inferior frontal gyrus; AMG: amygdala; OFC: orbitofrontal cortex; PCC: posterior cingulate cortex

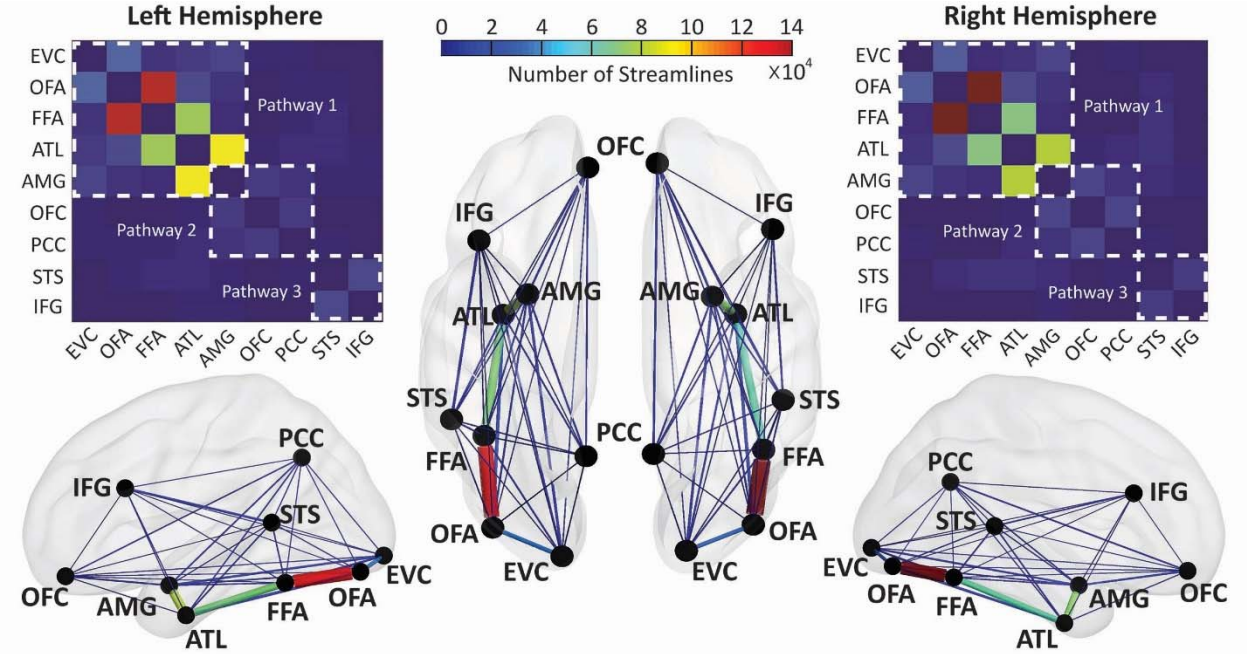


**Supplementary Figure 2. Pairwise Connection Strength (Streamline Counts) Between Face ROIs in Each Hemisphere.** Different from Fig 1 in the main text, here the connection strength was calculated by the number of streamlines between each pair of ROIs. Line thickness (as well as the color) is scaled to reflect the mean streamline count across all subjects. Similar to Fig 1, the streamline count patterns exhibit three distinct pathways: EVC-OFA-FFA-ATL-AMG (path 1), AMG-OFC-PCC (path2), and STS-IFG (path3),

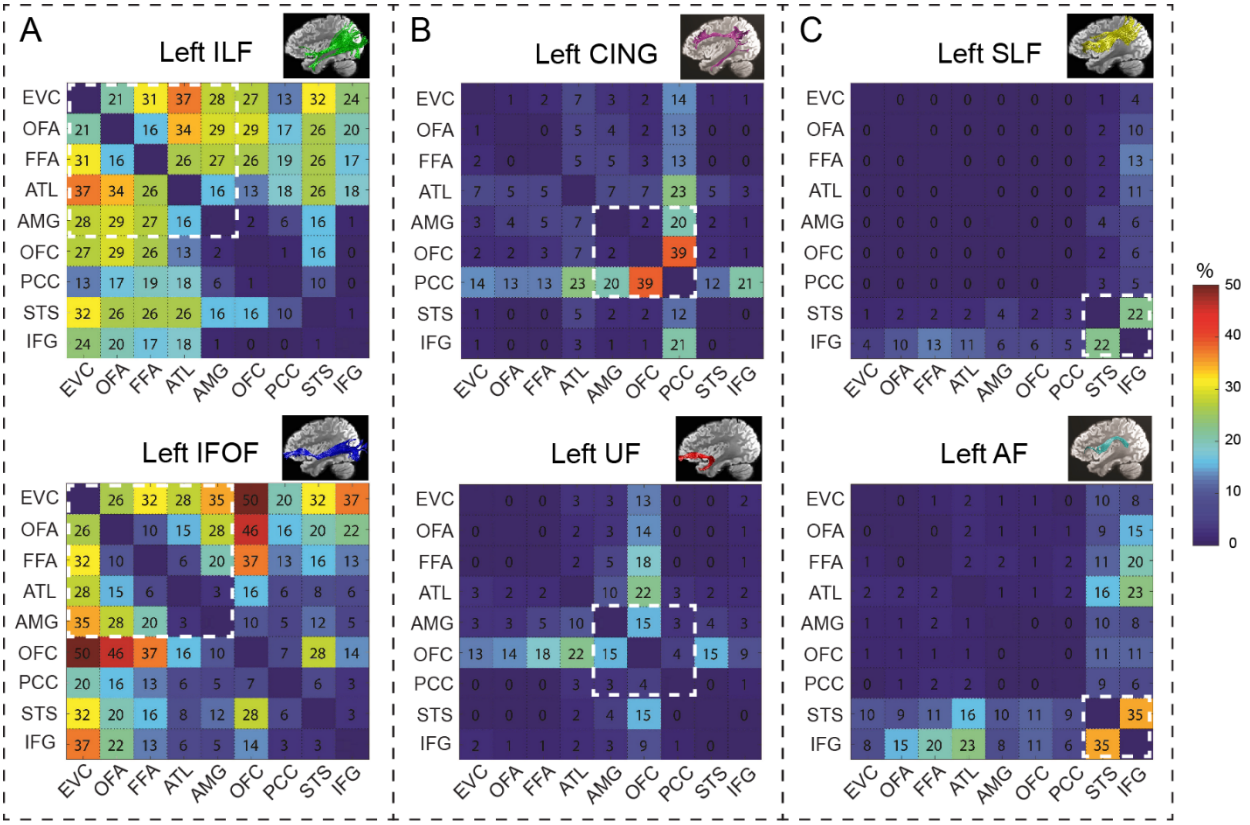


**Supplementary Figure 3. The Overlap Between Major White Matter Bundles and the Face Connectome in the Left Hemisphere.** Each number in the matrices represents the mean overlapped trajectories between an ROI-ROI tract and a major fasciculi across all subjects. Consistent with Fig 2 in the main text, we found that (A) the ventral pathway (EVC-OFA-FFA-ATL-AMG) was primarily contributed by the ILF and IFOF; (B) the medial pathway (AMG-OFC-PCC) was highly associated with the UF and CING; (C) the dorsal pathway (STS-IFG) was mostly supported by the SLF and AF;

Abbreviations: inferior longitudinal fasciculus (ILF), inferior fronto-occipital fasciculus (IFOF), superior longitudinal fasciculus (SLF), arcuate fasciculus (AF), uncinated fasciculus (UF), and cingulum (CING)

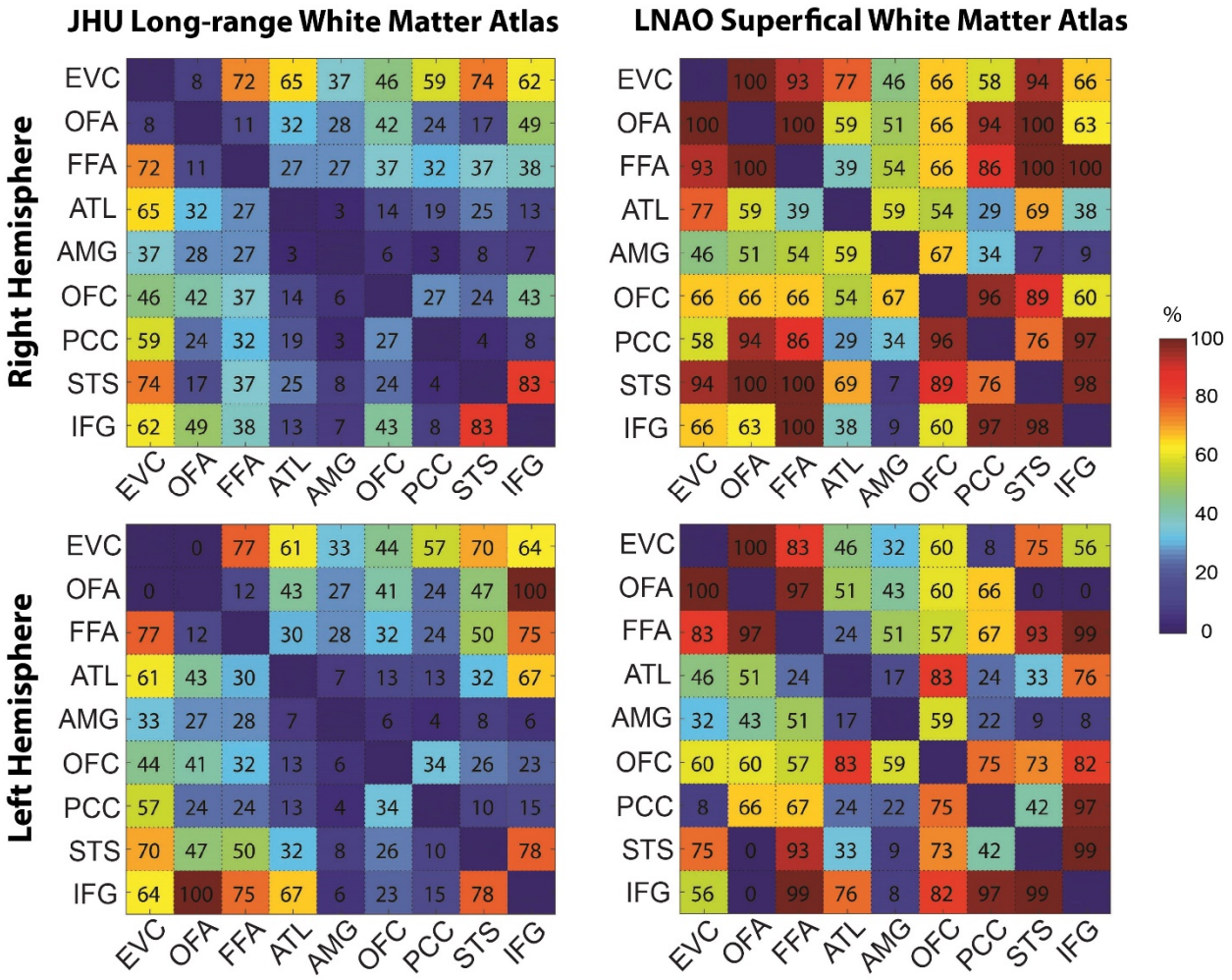


**Supplementary Figure 4. The relative contribution of large major bundles and superficial white matter to the structural connectome in each hemisphere**. Take the OFA-FFA connection as an example, 11% voxels in the right OFA-FFA (or 12% in the left OFA-FFA ) were overlapped with tracts in the JHU long-range white matter atlas, whereas all voxels in the right OFA-FFA (or 97% in the left OFA-FFA ) were overlapped with the LNAO superficial white matter atlas. For most ROI-ROI connections in the face network, they are mediated more by the superficial white matter system than the long-range fiber system.

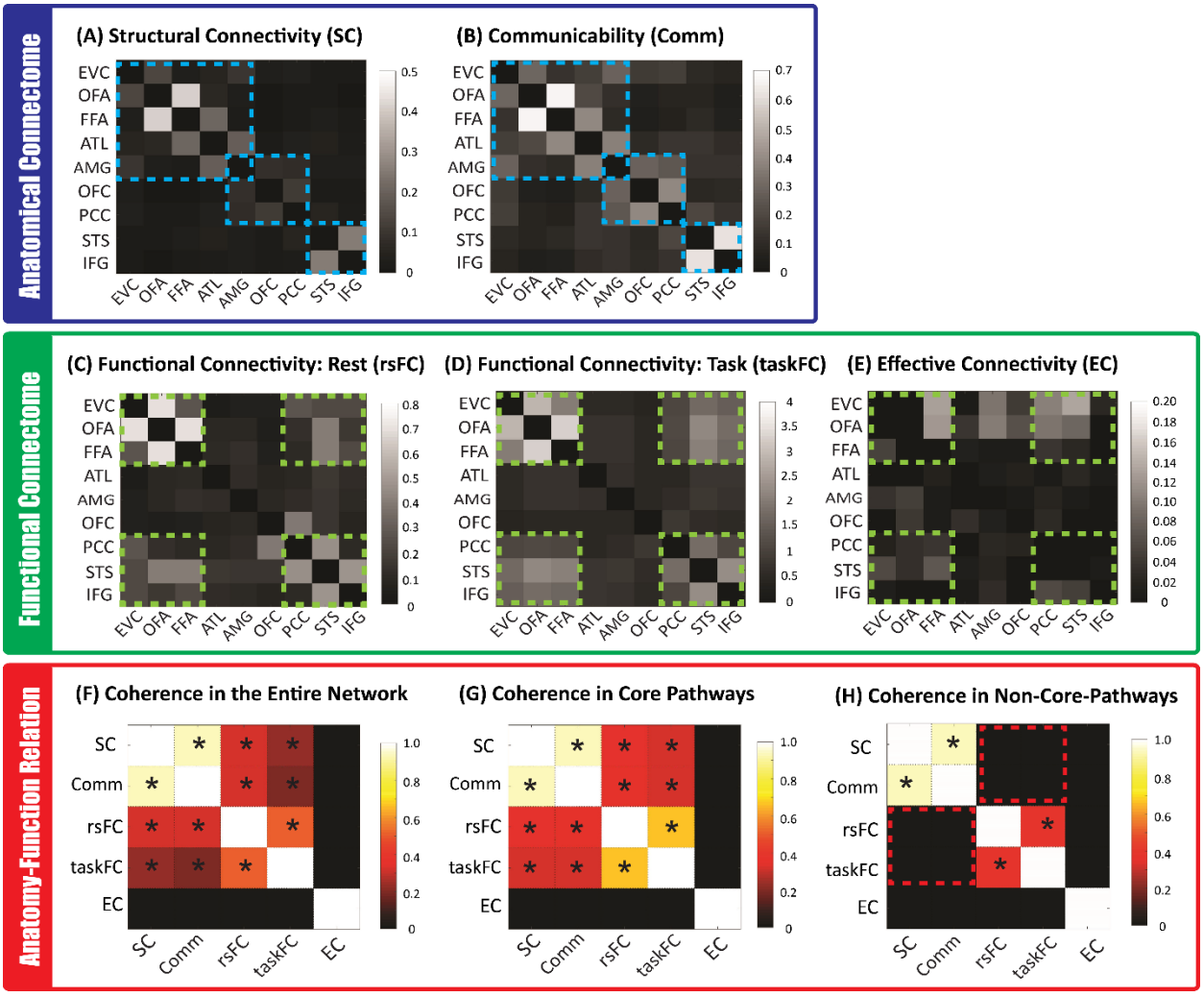


**Supplementary Figure 5. All Brain Connectivity Maps and Their Correspondence in the Left Hemisphere**. All information and symbols here can be similarly interpreted by the caption in Figure 3 in the main text.

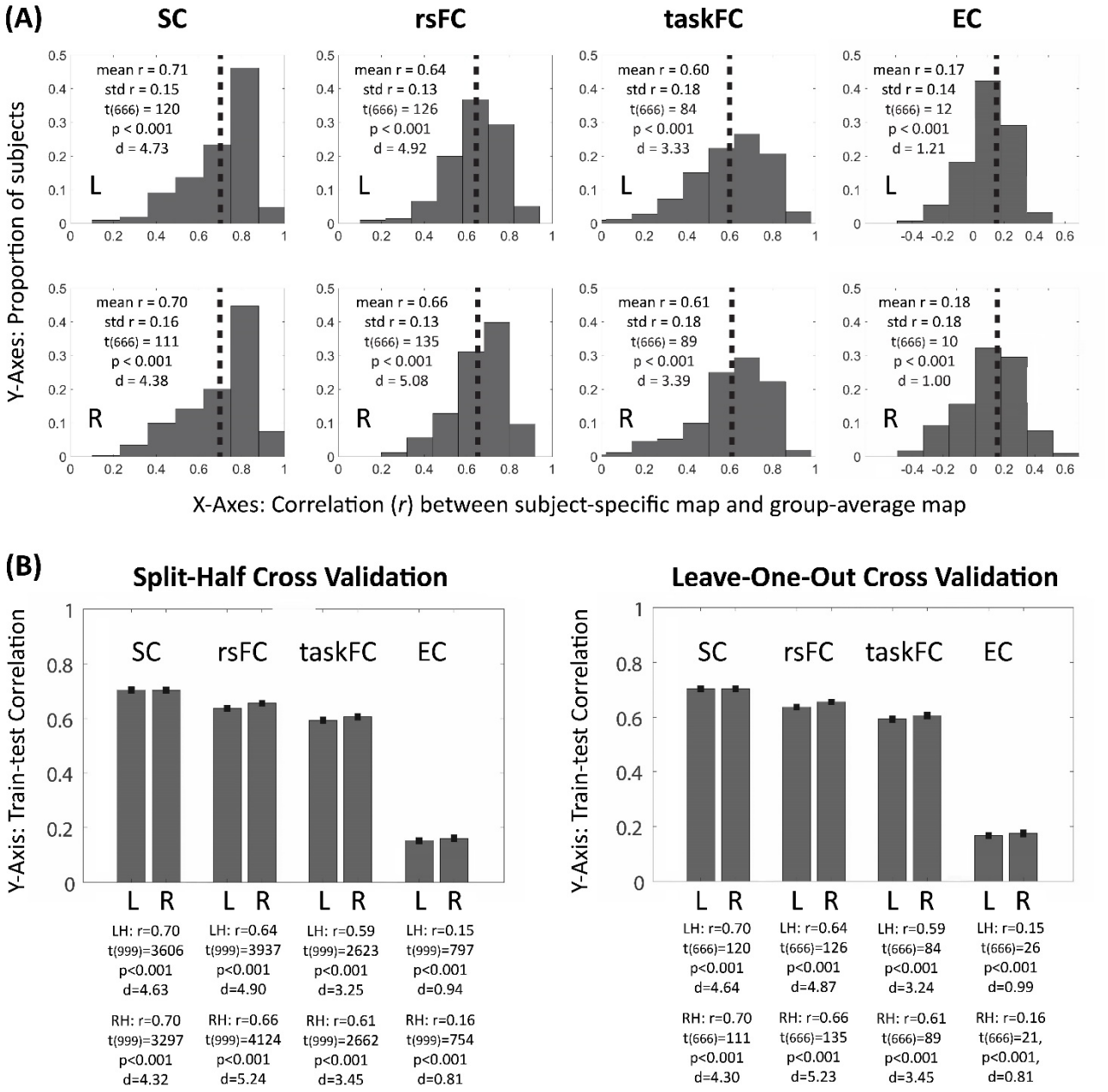


**Supplementary Figure 6. Individual Variance of the Face Connectome**. (A) For each subject, we calculated the similarity between group-averaged brain connectivity matrices (as those showed in Fig 3) and subject-specific ones. Histograms indicated that most subjects exhibited high group-to-individual similarity for the SC, rsFC and taskFC (i.e. over 75% subjects had *r* larger than 0.5) and moderate group-to-individual similarity for the EC (i.e. 67% subjects had *r* between 0.1 and 0.5). Dash line indicates mean group-to-individual correlation. (B) Two cross-validation (CV) analyses were further performed to measure group-to-group and group-to-individual similarity. The split-half CV randomly selected 50% subjects and used their averaged matrices to predict each of the rest 50% subject's matrices. This train-test procedure was repeated for 1000 times to calculate the overall subgroup-to-subgroup similarity. The leave-one-out CV (LOOCV) built group-averaged matrices from n-1 subjects and used them to predict the matrices in a new subject. This LOOCV train-test procedure was repeated for all 667 subjects to calculate the overall group-to-individual similarity. Consistent with the correlation distribution in (A), both CV schemes found very high train-test correlation for the SC, rsFC and taskFC and moderate train-test correlation for the EC. Error bar indicates standard error (SE).